

## Promoted Catalysis by Supported [Ru<sub>6</sub>N] Clusters in N<sub>2</sub> and/or H<sub>2</sub>: Structural and Chemical Controls

Yasuo Izumi\* and Ken-ichi Aika\*

Department of Environmental Chemistry and Engineering, Interdisciplinary Graduate School of Science and Engineering, Tokyo Institute of Technology, 4259 Nagatsuta, Midori-ku, Yokohama 226, Japan

Received: January 26, 1995; In Final Form: April 3, 1995<sup>®</sup>

Catalysis (ammonia synthesis) on supported nitrido clusters [Ru<sub>6</sub>N] was investigated as a potential catalysis system of transition metal + main group element in relation to the framework structure (change) of [Ru<sub>6</sub>N] clusters in H<sub>2</sub> or N<sub>2</sub> as found in the accompanying paper. The [Ru<sub>6</sub>N(μ-O)<sub>su</sub>]<sub>3</sub> (O<sub>su</sub>, oxygen atom at surface) clusters were prepared from the [Ru<sub>6</sub>N(CO)<sub>16</sub>]<sup>-</sup> cluster on MgO, K<sup>+</sup>-doped MgO, and Cs<sup>+</sup>-doped MgO, and the stability in reaction conditions of ammonia synthesis was probed by EXAFS (extended X-ray absorption fine structure). The reaction rates on these nitrido clusters were found to be faster than non-nitrido [Ru<sub>6</sub>] clusters prepared from [Ru<sub>6</sub>(CO)<sub>18</sub>]<sup>2-</sup>, degraded [Ru<sub>3</sub>(μ<sub>2</sub>-O)<sub>su</sub>]<sub>3</sub> clusters or aggregated Ru clusters (*N*<sub>Ru-Ru</sub> = 6.2–6.6) prepared from [Ru<sub>6</sub>N(CO)<sub>16</sub>]<sup>-</sup>, or conventional Ru catalysts. Also, the H<sub>2</sub>–D<sub>2</sub> exchange reactions (in the presence/absence of N<sub>2</sub>) proceeded faster on supported [Ru<sub>6</sub>N] clusters than the other catalysts. The Ru wt % dependence of ammonia synthesis activities on [Ru<sub>6</sub>N]/MgO suggested the importance of the Ru-hexamer ensemble and cluster/support interface for the catalysis. Related to the coordination structures of H or N<sub>2</sub> and structure changes of the [Ru<sub>6</sub>N] framework in H<sub>2</sub> or N<sub>2</sub> in the accompanying paper, the promoted reaction mechanism of ammonia synthesis on supported [Ru<sub>6</sub>N] clusters is discussed in terms of (1) nuclearity of Ru, (2) cluster/support interface, (3) structural effect through expansion/contraction of the [Ru<sub>6</sub>N] framework, and (4) electron donation by nitrido nitrogen, based on *in-situ* EXAFS, *in-situ* IR, H<sub>2</sub>–D<sub>2</sub> exchange reactions, reaction orders, and H/D isotope effects.

### Introduction

Compared to the simple structure and properties of the H<sub>2</sub> molecule, many unknown factors in the reaction mechanisms of hydrogenations on heterogeneous metal catalysts remain. There have been many studies on hydrogenations over heterogeneous catalysts on the molecular level for unsupported Ru metal<sup>1–8</sup> and supported Ru catalysts.<sup>1,9–12</sup> The reasons for complexity of hydrogenation are the weaker adsorption of H than the other small molecules,<sup>1,2</sup> the spillover from metal particle to support,<sup>9,10</sup> H-induced structure changes of active site,<sup>2,4</sup> etc.

We reported the [Ru<sub>6</sub>N(μ-O)<sub>su</sub>]<sub>x</sub> (O<sub>su</sub>, oxygen atom at surface) clusters on MgO, K<sup>+</sup>/MgO, and Cs<sup>+</sup>/MgO stabilized by nitrido nitrogen in the [Ru<sub>6</sub>] framework as catalysts for hydrogenation in the previous paper.<sup>13</sup> The number *x* varied according to the change of Ru wt %, 5–7 at Ru ~ 0.5 wt % and 3 at Ru ~ 2.5 wt %, and the [Ru<sub>6</sub>N] began to aggregate to larger particles at Ru ~ 4 wt % on the basis of the coordination number *N*<sub>Ru-O<sub>su</sub></sub> (*r*<sub>Ru-O<sub>su</sub></sub> = 2.09–2.20 Å) and *N*<sub>Ru-Ru</sub> (*r*<sub>Ru-Ru</sub> = 2.62–2.65 Å) by EXAFS. The dependence on Ru loading was interpreted as the difference of adsorption site of the [Ru<sub>6</sub>N(CO)<sub>16</sub>]<sup>-</sup> cluster on a MgO surface (MgO preheated at 773 K). The [Ru<sub>6</sub>N] cluster was suggested to be attached to a lower coordination site of the MgO surface at Ru ~ 0.5 wt %, compared to the interaction with relatively flat MgO planes at Ru ~ 2.5 wt %. The supported [Ru<sub>6</sub>N] clusters on MgO, K<sup>+</sup>/MgO, and Cs<sup>+</sup>/MgO had common structures with regard to cluster framework structure judging from the *N*<sub>Ru-Ru</sub> and *r*<sub>Ru-Ru</sub> obtained by EXAFS, but *not* with regard to Ru–O<sub>su</sub> bondings (metal/support interface).

H-induced structure changes were observed as the changes of *r*<sub>Ru-Ru</sub> (0.03–0.08 Å) for [Ru<sub>6</sub>N]/MgO and [Ru<sub>6</sub>N]–Cs<sup>+</sup>/

MgO by the adsorption/desorption of hydrogen. The hexamer [Ru<sub>6</sub>(μ-O)<sub>su</sub>]<sub>3–4</sub> on MgO without nitrido nitrogen prepared from the [Ru<sub>6</sub>C(CO)<sub>16</sub>Me]<sup>-</sup> cluster showed no H-induced change of *r*<sub>Ru-Ru</sub> (2.63 Å) in H<sub>2</sub>. Negligible structure changes were observed by the adsorption of molecular N<sub>2</sub> on [Ru<sub>6</sub>N]/MgO or [Ru<sub>6</sub>N]–Cs<sup>+</sup>/MgO. The study on the changes of catalytic performance should be useful for the better understanding of hydrogenation when the adsorption sites of [Ru<sub>6</sub>N] on MgO were varied at different Ru wt % and when supported clusters showed H-induced structure changes of the cluster framework [Ru<sub>6</sub>N]. The importance of hydrogen to the structure of the cluster and catalysis was reported in several catalyst systems. The palladium clusters Pd<sub>13</sub>(CO)<sub>x</sub> or Pd<sub>6</sub>(CO)<sub>y</sub> were suggested to be bonded to protons in the zeolite and formed an electron-deficient species [Pd<sub>n</sub>–H<sub>x</sub>]<sup>+•</sup>.<sup>14,15</sup> These catalysts were used in CO/H<sub>2</sub> reaction<sup>16</sup> and the hydrogenolysis of methylcyclopentene<sup>17</sup> or neopentene.<sup>18</sup> The effects of H<sub>2</sub> treatment on the structures of supported iridium clusters on MgO,<sup>19</sup> Al<sub>2</sub>O<sub>3</sub>,<sup>20</sup> or platinum clusters in zeolites<sup>21</sup> were reported. Two kinds of metal–O<sub>su</sub> (oxygen atom at surface) bondings were reported: 2.55–2.77 Å after reductions at lower temperatures (~573 K) and 2.19–2.24 Å after reductions at higher temperatures (~773 K). From the viewpoint of catalysis, the relations between cluster structure change and the hydrogenations have been investigated, and promoted reaction mechanisms on cluster sites were proposed for homogeneous<sup>22–24</sup> and heterogeneous catalysts.<sup>25</sup> The structural activations were reported for CH bonds of alkenes over [Rh<sub>2</sub>], [Ru<sub>3</sub>], or [Os<sub>3</sub>] clusters,<sup>22</sup> carbon monoxide over a [Ru<sub>3</sub>] cluster<sup>23</sup> or [Ru<sub>2</sub>] complex,<sup>24</sup> and the OH bond of ethanol over [MoO<sub>2</sub>(μ-O)<sub>2</sub>]<sub>2</sub>/SiO<sub>2</sub> or [NbO(μ-O)<sub>3</sub>]<sub>2</sub>/SiO<sub>2</sub>.<sup>25</sup>

In this paper, we report the promoted ammonia synthesis on supported [Ru<sub>6</sub>N] clusters and the contributions of nuclearity of clusters, cluster support interface, structure change of [Ru<sub>6</sub>N] cluster framework, and chemical effect of nitrido nitrogen to catalysis. Six-Ru-atom clusters without an interstitial atom

\* To whom correspondence should be addressed. E-mail: yizumi@chemenv.titech.ac.jp.

<sup>®</sup> Abstract published in *Advance ACS Abstracts*, June 1, 1995.

[Ru<sub>6</sub>(CO)<sub>18</sub>]<sup>2-</sup>, the carbido cluster [Ru<sub>6</sub>C(CO)<sub>16</sub>Me]<sup>-</sup>, and conventional impregnated Ru catalysts were employed as comparisons.

### Experimental Section

Supported clusters were prepared in a manner similar to that in a previous paper.<sup>13</sup> Briefly, [PPN]<sup>+</sup>[Ru<sub>6</sub>N(CO)<sub>16</sub>]<sup>-</sup> (**1**) (PPN = N(PPH<sub>3</sub>)<sub>2</sub>) ([PPN]<sup>+</sup>Cl<sup>-</sup>, Aldrich Chem Co., 97%; NaN<sub>3</sub>, Wako Pure Chemical Ind., >90%; Ru<sub>3</sub>(CO)<sub>12</sub>, Soekawa) was supported on MgO, K<sup>+</sup>/MgO, Cs<sup>+</sup>/MgO, or Al<sub>2</sub>O<sub>3</sub> by reaction at 290 K (1 h) in purified THF (tetrahydrofuran, Wako, Special Grade) in Ar (99.99%). MgO was prepared from Mg(OH)<sub>2</sub> (Wako, 99.99%) by heating at 773 K (2 h) in vacuum. A water solution of Cs<sub>2</sub>CO<sub>3</sub> (Wako, >95%) or K<sub>2</sub>CO<sub>3</sub> (Wako, >99.5%) was impregnated onto MgO, followed by treatments in O<sub>2</sub> and then in H<sub>2</sub> at 773 K. Al<sub>2</sub>O<sub>3</sub> (aerosil C) was treated at 623 K (2 h) in vacuum ([Ru<sub>6</sub>N]/oxide). [PPN]<sup>+</sup><sub>2</sub>[Ru<sub>6</sub>(CO)<sub>18</sub>]<sup>2-</sup> (**2**) or [NMe<sub>3</sub>CH<sub>2</sub>Ph]<sup>+</sup>[Ru<sub>6</sub>C(CO)<sub>16</sub>Me]<sup>-</sup> (**3**) ([NMe<sub>3</sub>CH<sub>2</sub>Ph]<sup>+</sup>Cl<sup>-</sup>, Wako; CH<sub>3</sub>I, Wako, Special Grade) was supported on MgO in THF solution in a manner similar to the case of **1** ([Ru<sub>6</sub>]/MgO and [Ru<sub>6</sub>C]/MgO). As pretreatment, incipient supported clusters were heated in vacuum at 813 K except for [Ru<sub>6</sub>N]-Cs<sup>+</sup>/MgO and [Ru<sub>6</sub>N]-K<sup>+</sup>/MgO at 673 K, followed by treatment in H<sub>2</sub> for 1 h (*T*<sub>H<sub>2</sub></sub> = 588–773 K). Thus-prepared samples are denoted as cluster/oxide-*x*H (*x*, temperature/K in H<sub>2</sub>). The conventional Ru/MgO, Ru-Cs<sup>+</sup>/MgO (Cs<sup>+</sup>/Ru = 2.0 in atomic ratio), and Ru/Al<sub>2</sub>O<sub>3</sub> catalysts were prepared from a solution of Ru(NO)(NO<sub>3</sub>)<sub>3</sub> (N. E. Chemcat, Ru 5 g L<sup>-1</sup>). They were heated in O<sub>2</sub> and then in H<sub>2</sub> at 773 K before used as catalysts. The Ru loadings were 2.5 wt % on MgO, K<sup>+</sup>/MgO, Cs<sup>+</sup>/MgO and 1.6 wt % on Al<sub>2</sub>O<sub>3</sub> except for experiments of weight percent dependence for MgO-supported clusters (0.48–3.9 wt %). The descriptions without special notation for catalysts on MgO were for samples at 2.5 wt % Ru.

The ammonia synthesis reactions were carried out under 101 kPa of reaction gas (*P*<sub>N<sub>2</sub></sub>/*P*<sub>H<sub>2</sub></sub> = 1/3) at 588 K in a flow system (flow rate 60 cm<sup>3</sup> min<sup>-1</sup>). Produced ammonia was analyzed by the decrease of electron conductivity (1.7–0.8 mS cm<sup>-1</sup>) of the H<sub>2</sub>SO<sub>4</sub> solution (0.004–0.002 N). The linearity of the correlation between the produced NH<sub>3</sub> amount and the decrease of electron conductivity was checked before observation.<sup>26</sup> The reaction temperature was chosen to be relatively low (588 K) to realize differential (*not* near equilibrium) working conditions in kinetic measurements based on the thermodynamics; that is, the equilibrium value for ammonia synthesis was calculated from the Gibbs free energy to be 1.7 and 0.45% of NH<sub>3</sub> at 588 and 673 K, respectively, compared to the highest values of N<sub>2</sub>–H<sub>2</sub> conversion in the case of the most active [Ru<sub>6</sub>N]-Cs<sup>+</sup>/MgO (0.046 and 0.44% at 588 and 673 K, respectively, 0.070 g of cluster catalyst used). The rates of H<sub>2</sub>–D<sub>2</sub> exchange reaction were monitored in a closed circulating system (dead volume 100 cm<sup>3</sup>) connected with a mass spectrometer (ANELVA NAG515) with 6.7 kPa of H<sub>2</sub> and 6.7 kPa of D<sub>2</sub> at 273 K. The same reactions were also carried out in the presence of 4.5 kPa of N<sub>2</sub>. The reverse reactions of the N<sub>2</sub>–H<sub>2</sub> reaction, the decomposition reaction of ammonia, were carried out in the closed circulating system with 1.3 kPa of NH<sub>3</sub> and 76.0 kPa of H<sub>2</sub> at 588 K. Produced N<sub>2</sub> was detected by GC (Shimadzu GC8A) with a Unibeads C (GL Science) column at 433 K.

The EXAFS spectra of the Ru K edge were measured for these supported clusters at the beamline 10B and 6B (2.5 GeV, current 360–260 A) of the Photon Factory (PF) in the National Laboratory for High Energy Physics (Proposal No. 93G010) between June 1993 and November 1994. The sample was transferred to an EXAFS Pyrex cell with Kapton films on both sides by using the Schlenk technique from a closed circulating system for sample preparation. The data collection was performed at 30–293 K utilizing a closed cycle refrigerator

(Cryo System, LTS-21). The procedure of data analysis was described in the accompanying paper.<sup>13</sup>

FTIR spectra of supported Ru clusters were recorded on a FTIR spectrometer (JASCO FTIR-5000) in a quartz IR cell with NaCl windows on both sides, combined with a closed circulating system. Support oxide disks were treated in the same conditions as powders in the IR cell and impregnated by a drop of a THF solution of the Ru clusters. The temperature of the IR cell can be controlled at 193–295 K by a tube wound around the cell (cooled by liquid nitrogen by using a rotary pump) and at 295–823 K by a heating coil wound around the cell. H<sub>2</sub> (99.99%) and N<sub>2</sub> (99.99%) gas were purchased from Toyo Sanso Co., Ltd. The impurities (as molecular content) were less than the following values: H<sub>2</sub>O < 10, N<sub>2</sub> < 50, O<sub>2</sub> < 10, CO < 10, CO<sub>2</sub> < 10 ppm, and total hydrocarbons < 10 ppm (as carbon content) in the H<sub>2</sub> gas, and H<sub>2</sub>O < 10, O<sub>2</sub> < 2 ppm, and total hydrocarbons < 1 ppm (as carbon content) in the N<sub>2</sub> gas. D<sub>2</sub> and <sup>15</sup>N<sub>2</sub> gas were purchased from Syoko Co., Ltd. The deuterium content in total hydrogen was >99.8% for the D<sub>2</sub> gas, and impurities (as molecular content) were less than the following values: HD < 4000, H<sub>2</sub>O < 10, N<sub>2</sub> < 50, O<sub>2</sub> < 10, CO < 10, CO<sub>2</sub> < 10 ppm, and total hydrocarbons < 10 ppm (as carbon content). The <sup>15</sup>N atom content in total nitrogen was 99.3% for <sup>15</sup>N<sub>2</sub> gas. The purity was on the same level as <sup>14</sup>N<sub>2</sub>. The gas for adsorption (H<sub>2</sub> and N<sub>2</sub>) was again purified by a liquid nitrogen trap before each measurement.

The hydrogen and nitrogen uptake measurements were carried out in a small space (30 cm<sup>3</sup>) in a closed circulation system connected to the manometer. The temperature of the samples was maintained in liquid N<sub>2</sub> (77 K), dry ice + liquid N<sub>2</sub> + acetone (179 K), or ice (273 K). The uptake on Ru at 77–179 K was calculated by subtracting the observed uptake on Ru-free oxide from the observed uptake on the Ru-supported sample. The Ru-free support oxides, MgO, Cs<sup>+</sup>/MgO, or Al<sub>2</sub>O<sub>3</sub>, were pretreated in the same conditions as corresponding Ru cluster catalysts.

### Results

**Promoted Ammonia Synthesis on Supported [Ru<sub>6</sub>N] Clusters.** We observed ammonia synthesis reactions on supported nitrido ruthenium clusters and related Ru catalysts at 588 K in 25.3 kPa of N<sub>2</sub> and 76.0 kPa of H<sub>2</sub> (Table 1 (A)). The observed turnover frequencies (TOFs) were estimated per [Ru<sub>6</sub>N] (*or* [Ru<sub>6</sub>]) cluster for supported clusters and per surface Ru atoms estimated from the Ru dispersion (H/Ru) by hydrogen adsorption at 273 K for conventional Ru/MgO, Ru-Cs<sup>+</sup>/MgO, and Ru/Al<sub>2</sub>O<sub>3</sub> (H/Ru were 0.13, 0.10, and 0.037, respectively).

The TOFs of supported nitrido-Ru clusters on MgO, K<sup>+</sup>/MgO, or Cs<sup>+</sup>/MgO treated in H<sub>2</sub> at 588 K (0.11–0.40 min<sup>-1</sup>) were superior to the conventional Ru/MgO (0.002 min<sup>-1</sup>) or the Ru catalysts in the literature on the TOF or product h<sup>-1</sup> g<sub>cat</sub><sup>-1</sup> basis. The turnovers of [Ru<sub>6</sub>N] on MgO, K<sup>+</sup>/MgO, and Cs<sup>+</sup>/MgO corresponded to 13–48 NH<sub>3</sub> per [Ru<sub>6</sub>N] cluster (in mol) in 2 h, excluding the possibility of unusually high activity due to hydrogenation of nitrogen atoms native to supported nitrido clusters.

The TOF on [Ru<sub>6</sub>N]-Cs<sup>+</sup>/MgO-588H (0.40 min<sup>-1</sup>) corresponds to 9.9 × 10<sup>-4</sup> mol-NH<sub>3</sub> h<sup>-1</sup> g<sub>cat</sub><sup>-1</sup>, larger than 0.0071 min<sup>-1</sup> on conventional K<sup>+</sup>-Ru/TiO<sub>2</sub> (7 wt % Ru, K<sup>+</sup>/Ru = 1/10, 101 kPa),<sup>27</sup> 0.06 min<sup>-1</sup> on Ru/zeolite KX at 623 K (2 wt % Ru, 101 kPa),<sup>28</sup> 6.9 × 10<sup>-4</sup> mol-NH<sub>3</sub> h<sup>-1</sup> g<sub>cat</sub><sup>-1</sup> on conventional Ru-Cs<sup>+</sup>/MgO at 588 K (2 wt % Ru, Cs<sup>+</sup>/Ru = 1.0, 80 kPa),<sup>26</sup> or others.<sup>29</sup> The dependence of activities for [Ru<sub>6</sub>N]/oxides on the kind of support was Cs<sup>+</sup>/MgO (0.40 min<sup>-1</sup>) > K<sup>+</sup>/MgO (0.19) > MgO (0.11) ≫ Al<sub>2</sub>O<sub>3</sub> (0) when these cluster catalysts were pretreated in H<sub>2</sub> at 588 K. The [Ru<sub>6</sub>N]/Al<sub>2</sub>O<sub>3</sub> exhibited no activities after the H<sub>2</sub> treatment at

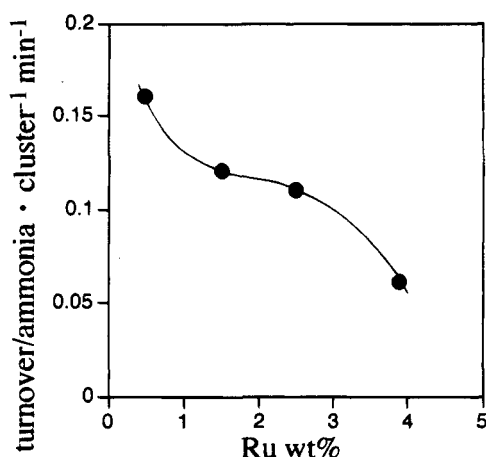
**TABLE 1: Turnover Frequencies (TOFs)<sup>a</sup> (product cluster<sup>-1</sup> min<sup>-1</sup>) of Ammonia Synthesis (A), Decomposition (B), H<sub>2</sub>-D<sub>2</sub> Exchange (C) Reactions on Supported [Ru<sub>6</sub>N(CO)<sub>16</sub>]<sup>-</sup>, [Ru<sub>6</sub>C(CO)<sub>16</sub>Me]<sup>-</sup>, or [Ru<sub>6</sub>(CO)<sub>18</sub>]<sup>2-</sup> Clusters, and Conventional Ru Catalysts**

reaction condition	(A)	(C)	(C')	(B)
<i>T</i> <sub>reac</sub> /K	588	273	273	588
<i>P</i> <sub>N<sub>2</sub></sub> /kPa	25.3		4.5	
<i>P</i> <sub>H<sub>2</sub></sub> /kPa	76.0	6.7	6.7	76.0
<i>P</i> <sub>D<sub>2</sub></sub> /kPa		6.7	6.7	
<i>P</i> <sub>NH<sub>3</sub></sub> /kPa				1.3

sample	structure formulation	<i>T</i> <sub>H<sub>2</sub></sub> /K	TOF			
[Ru <sub>6</sub> N(CO) <sub>16</sub> ] <sup>-</sup> /MgO	[Ru <sub>6</sub> N(μ-O <sub>su</sub> ) <sub>3</sub> ]	588	0.11	160	22	0.001
	aggregated ( <i>N</i> <sub>Ru-Ru</sub> = 6.6)	773	0.017	58	21	
[Ru <sub>6</sub> N(CO) <sub>16</sub> ] <sup>-</sup> -K <sup>+</sup> /MgO	[Ru <sub>6</sub> N(μ-O <sub>su</sub> ) <sub>3</sub> ]	588	0.19			0.018
[Ru <sub>6</sub> N(CO) <sub>16</sub> ] <sup>-</sup> -Cs <sup>+</sup> /MgO	[Ru <sub>6</sub> N(μ-O <sub>su</sub> ) <sub>3</sub> ]	588	0.40	110	60	
[Ru <sub>6</sub> C(CO) <sub>16</sub> Me] <sup>-</sup> /MgO	[Ru <sub>6</sub> (μ-O <sub>su</sub> ) <sub>3-4</sub> ]	623	0.018	42		
[Ru <sub>6</sub> (CO) <sub>18</sub> ] <sup>2-</sup> /MgO	aggregated ( <i>N</i> <sub>Ru-Ru</sub> = 6.2)	588	0.013	42		
conv. Ru/MgO		773	0.002	0.013	0.016	
conv. Ru-Cs <sup>+</sup> /MgO		773	0.017			
[Ru <sub>6</sub> N(CO) <sub>16</sub> ] <sup>-</sup> /Al <sub>2</sub> O <sub>3</sub>	[Ru <sub>3</sub> (μ <sub>2</sub> -O <sub>su</sub> ) <sub>3</sub> ]	588	0	2.0		
conv. Ru/Al <sub>2</sub> O <sub>3</sub>		773	0.001			

<sup>a</sup> In the units (product surface Ru<sup>-1</sup> min<sup>-1</sup>) for conventional Ru catalysts based on the uptake (H/Ru) measurements.



**Figure 1.** Ru wt % dependence of turnover frequencies (product cluster<sup>-1</sup> min<sup>-1</sup>) of ammonia synthesis: reaction temperature 588 K, flow rate 60 cm<sup>3</sup> min<sup>-1</sup>, *P*<sub>N<sub>2</sub></sub> = 25.3 kPa, *P*<sub>H<sub>2</sub></sub> = 76.0 kPa.

588–773 K, although conventional Ru/Al<sub>2</sub>O<sub>3</sub> slowly produced ammonia (0.001 min<sup>-1</sup>).

The control experiments were performed for the supported Ru cluster prepared from [Ru<sub>6</sub>(CO)<sub>18</sub>]<sup>2-</sup> which did not have interstitial nitrogen in the [Ru<sub>6</sub>] framework. The TOF was 0.013 min<sup>-1</sup>, only 12% of that of the corresponding supported nitrido cluster (0.11 min<sup>-1</sup>) (Table 1). However, the [Ru<sub>6</sub>] framework of [Ru<sub>6</sub>]/MgO was aggregated to larger particles (*N*<sub>Ru-Ru</sub> = 6.2) by heating in vacuum (813 K), and in H<sub>2</sub> (588 K).<sup>13</sup> The [Ru<sub>6</sub>-(μ-O<sub>su</sub>)<sub>3-4</sub>] species can be prepared from cluster 3 by heating in vacuum and in H<sub>2</sub> at 623 K.<sup>13,30</sup> The activity was 0.018 min<sup>-1</sup> (Table 1), still smaller than that of [Ru<sub>6</sub>N]/MgO. It should be noted that the activity on [Ru<sub>6</sub>N]/MgO had strong dependence on the pretreatment temperature in H<sub>2</sub> (*T*<sub>H<sub>2</sub></sub>). The TOF on [Ru<sub>6</sub>N]/MgO-773H (0.017 min<sup>-1</sup>) was only 15% of that on [Ru<sub>6</sub>N]/MgO-588H (Table 1), whereas the dependence on *T*<sub>H<sub>2</sub></sub> was not observed for [Ru<sub>6</sub>]/MgO or [Ru<sub>6</sub>(μ-O<sub>su</sub>)<sub>3-4</sub>] on MgO when treated in H<sub>2</sub> at 588–773 K.

The dependence of ammonia synthesis rates on Ru wt % was shown in Figure 1 for [Ru<sub>6</sub>N]/MgO-588H catalysts. The TOF was not varied so much around 1.5–3 wt % Ru (0.10–0.12 min<sup>-1</sup>). The increase at lower Ru loading (0.48 wt % Ru) by about 30% and the decrease at higher Ru loading (3.9 wt %) by about 45% were observed.

**Inverse Hydrogen Isotope Effects in Ammonia Synthesis on Supported [Ru<sub>6</sub>N] Clusters.** The H/D isotope effects in N<sub>2</sub>-H<sub>2</sub> reactions were observed for [Ru<sub>6</sub>N]/MgO-588H, [Ru<sub>6</sub>N]-

**TABLE 2: Hydrogen Isotope Effects for Ammonia Synthesis on [Ru<sub>6</sub>N(CO)<sub>16</sub>]<sup>-</sup>/MgO, [Ru<sub>6</sub>N(CO)<sub>16</sub>]<sup>-</sup>-Cs<sup>+</sup>/MgO, and Conventional Ru/MgO<sup>a</sup>**

sample	structure formulation	<i>T</i> <sub>H<sub>2</sub></sub>	<i>r</i> <sub>D<sub>2</sub></sub> / <i>r</i> <sub>H<sub>2</sub></sub>
[Ru <sub>6</sub> N(CO) <sub>16</sub> ] <sup>-</sup> /MgO	[Ru <sub>6</sub> N(μ-O <sub>su</sub> ) <sub>3</sub> ]	588	1.4
[Ru <sub>6</sub> N(CO) <sub>16</sub> ] <sup>-</sup> -Cs <sup>+</sup> /MgO	[Ru <sub>6</sub> N(μ-O <sub>su</sub> ) <sub>3</sub> ]	588	1.5
conv. Ru/MgO		773	1.0

<sup>a</sup> Reaction temperature 588 K. *P*<sub>N<sub>2</sub></sub> = 25.3, *P*<sub>H<sub>2</sub></sub> (or *P*<sub>D<sub>2</sub></sub>) = 76.0 kPa.

Cs<sup>+</sup>/MgO-588H, and conventional Ru/MgO at 101 kPa (N<sub>2</sub> 25.3, H<sub>2</sub> (or D<sub>2</sub>) 76.0 kPa) (reaction temperature 588 K). The ratio (*r*<sub>D<sub>2</sub></sub>/*r*<sub>H<sub>2</sub></sub>) was 1.4 for [Ru<sub>6</sub>N]/MgO, 1.5 for [Ru<sub>6</sub>N]-Cs<sup>+</sup>/MgO, and 1.0 (no isotope effect) for conventional Ru/MgO (Table 2).

**H<sub>2</sub>-D<sub>2</sub> Exchange Reactions in the Presence/Absence of N<sub>2</sub>.** H<sub>2</sub>-D<sub>2</sub> exchange reactions were carried out in H<sub>2</sub> (6.7 kPa) + D<sub>2</sub> (6.7 kPa) or in H<sub>2</sub> (6.7 kPa) + D<sub>2</sub> (6.7 kPa) + N<sub>2</sub> (4.5 kPa) at 273 K. The TOFs of H<sub>2</sub>-D<sub>2</sub> exchange reaction in H<sub>2</sub> + D<sub>2</sub> were in the order [Ru<sub>6</sub>N]/MgO-588H (160 min<sup>-1</sup>) > [Ru<sub>6</sub>N]-Cs<sup>+</sup>/MgO-588H (110) > [Ru<sub>6</sub>N]/MgO-773H (58) ~ [Ru<sub>6</sub>]/MgO-588H (42) ~ [Ru<sub>6</sub>C]/MgO-623H (42) ≫ [Ru<sub>6</sub>N]/Al<sub>2</sub>O<sub>3</sub> (2.0) ≫ conventional Ru/MgO (0.013) (Table 1 (C)). The TOF on [Ru<sub>6</sub>N]/MgO or [Ru<sub>6</sub>N]-Cs<sup>+</sup>/MgO was faster than aggregated Ru clusters or [Ru(μ-O<sub>su</sub>)<sub>3-4</sub>] on MgO (without nitrido N) by 2–4 times, than [Ru<sub>6</sub>N]/Al<sub>2</sub>O<sub>3</sub> on the order of 2, and than conventional Ru/MgO on the order of 3. The TOFs of H<sub>2</sub>-D<sub>2</sub> exchange reaction in H<sub>2</sub> + D<sub>2</sub> + N<sub>2</sub> were in the order [Ru<sub>6</sub>N]-Cs<sup>+</sup>/MgO-588H (60 min<sup>-1</sup>) > [Ru<sub>6</sub>N]/MgO-588H (22) ~ [Ru<sub>6</sub>N]/MgO-773H (21) ≫ conventional Ru/MgO (0.016) (Table 1 (C')). The decreased ratios of the H<sub>2</sub>-D<sub>2</sub> exchange rate by the addition of N<sub>2</sub> were 0.14 for [Ru<sub>6</sub>N]/MgO-588H, 0.55 for [Ru<sub>6</sub>N]-Cs<sup>+</sup>/MgO-588H, and 0.36 for [Ru<sub>6</sub>N]/MgO-773H compared to the smaller change for conventional Ru/MgO (1.2).

**Other Kinetic Measurements for Supported [Ru<sub>6</sub>N] Clusters and Conventional Ru/MgO.** The pressure dependence was observed by changing the pressures of N<sub>2</sub> and H<sub>2</sub> independently (*P*<sub>N<sub>2</sub></sub> = 12.7–25.3 kPa, *P*<sub>H<sub>2</sub></sub> = 38.0–76.0 kPa). The apparent reaction orders of the N<sub>2</sub>-H<sub>2</sub> reactions were 0.78 and 0.20 on [Ru<sub>6</sub>N]/MgO-588H and 0.89 and 0.18 on [Ru<sub>6</sub>N]-Cs<sup>+</sup>/MgO-588H for *P*<sub>N<sub>2</sub></sub> and *P*<sub>H<sub>2</sub></sub>, respectively.

The decomposition rates of NH<sub>3</sub> (1.8 kPa) in H<sub>2</sub> (76.0 kPa) were observed for [Ru<sub>6</sub>N]/MgO-588H and [Ru<sub>6</sub>N]-Cs<sup>+</sup>/MgO-588H at 588 K (Table 1 (B)). This reverse reaction proceeded slower on the order of 1–2 magnitudes than the forward (synthesis) reaction.

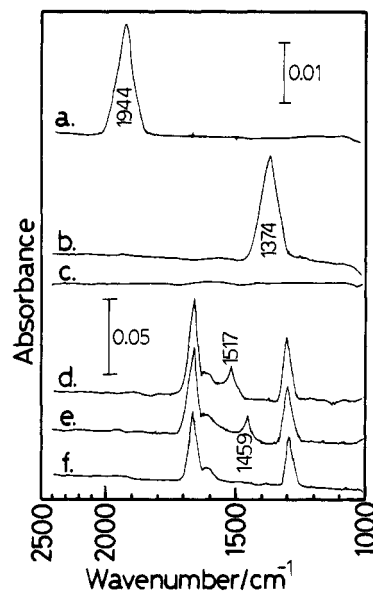


**Figure 2.** IR spectra of (a) [Ru<sub>6</sub>N]/MgO in H<sub>2</sub> (23.3 kPa), (b) [Ru<sub>6</sub>N]/MgO in D<sub>2</sub> (23.3 kPa), (c) MgO in H<sub>2</sub> (23.3 kPa), (d) [Ru<sub>6</sub>N]/MgO in <sup>14</sup>N<sub>2</sub> (23.3 kPa), (e) [Ru<sub>6</sub>N]/MgO in <sup>15</sup>N<sub>2</sub> (23.3 kPa), and (f) MgO in <sup>14</sup>N<sub>2</sub> (23.3 kPa). Each background spectrum was for the sample before the introduction of gas. Observed temperature = 193 K. [Ru<sub>6</sub>N]/MgO was evacuated at 813 K and in H<sub>2</sub> at 588 K. MgO was evacuated at 813 K.

**TABLE 3: Amount of Gas Uptake on the Supported [Ru<sub>6</sub>N(CO)<sub>16</sub>]<sup>-</sup> Clusters**

sample	<i>T</i> <sub>adsorption</sub> /K	number of H(a) or N <sub>2</sub> (a) per [Ru <sub>6</sub> N]	
		H(a)	N <sub>2</sub> (a)
[Ru <sub>6</sub> N]/MgO	uptake <sup>a</sup>	179	4.0
	IR intensity <sup>b</sup>	193	3.1
[Ru <sub>6</sub> N]-Cs <sup>+</sup> /MgO	uptake <sup>a</sup>	77	5.2
	uptake <sup>a</sup>	179	0.7
[Ru <sub>6</sub> N]/Al <sub>2</sub> O <sub>3</sub>	uptake <sup>a</sup>	179	1.9 <sup>c</sup>
	IR intensity <sup>b</sup>	193	0

<sup>a</sup> By manometer, in H<sub>2</sub> (76 kPa) or N<sub>2</sub> (25 kPa). The uptake on Ru was calculated by subtracting the observed uptake on MgO, Cs<sup>+</sup>/MgO, or Al<sub>2</sub>O<sub>3</sub> from the observed uptake on [Ru<sub>6</sub>N]/MgO, [Ru<sub>6</sub>N]-Cs<sup>+</sup>/MgO, or [Ru<sub>6</sub>N]/Al<sub>2</sub>O<sub>3</sub>, respectively. <sup>b</sup> Calculated from the IR peak area in H<sub>2</sub> (23.3 kPa) compared to  $\nu_{\text{Ru-H}}$  for H(a) on a conventional Ru/MgO sample. <sup>c</sup> 1.9/2 per [Ru<sub>3</sub>].

### IR Spectra for Supported [Ru<sub>6</sub>N] Clusters in H<sub>2</sub> or in N<sub>2</sub>.

**1. [Ru<sub>6</sub>N]/MgO.** Figure 2a shows the IR spectrum observed at 193 K for 30 min in H<sub>2</sub> (23.3 kPa) for [Ru<sub>6</sub>N]/MgO-588H (also in the case of the following IR spectra, the background spectrum was for the sample before introduction of gas). A strong peak at 1944 cm<sup>-1</sup> in Figure 2a was shifted to 1374 cm<sup>-1</sup> by evacuating the H<sub>2</sub> and introducing D<sub>2</sub> (23.3 kPa) (Figure 2b). In contrast to these peaks on [Ru<sub>6</sub>N]/MgO, no peak was observed on MgO in H<sub>2</sub> (23.3 kPa) (Figure 2c). The ratio of the wavenumber in D<sub>2</sub> and in H<sub>2</sub> (0.707) on [Ru<sub>6</sub>N]/MgO was similar to the theoretical ratio  $\nu_{\text{Ru-D}}/\nu_{\text{Ru-H}}$  (0.711). The amount of H(a) was estimated to be 3.1 per [Ru<sub>6</sub>N] cluster (Table 3) on the basis of the intensity of the  $\nu_{\text{Ru-H}}$  peak compared to the corresponding peak of H(a) on conventional Ru/MgO, assuming the absorption coefficients were the same between the two. The molar ratio H/[Ru<sub>6</sub>N] was 4.0 by uptake measurement at 179 K (Table 3).

<sup>14</sup>N<sub>2</sub> (23.3 kPa) was introduced to [Ru<sub>6</sub>N]/MgO-588H at 193 K. The IR spectrum after 30 min in N<sub>2</sub> is shown in Figure 2d. Two peaks at 1605(w, sh) and 1517(m) cm<sup>-1</sup> were observed in addition to strong peaks at 1664 and 1308 cm<sup>-1</sup>. In the corresponding spectrum in <sup>15</sup>N<sub>2</sub> (23.3 kPa) (Figure 2e), the peak at 1517 cm<sup>-1</sup> was shifted to 1459 cm<sup>-1</sup>, while the other three

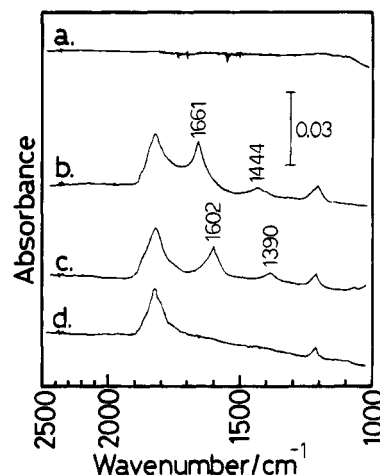


**Figure 3.** IR spectra of (a) [Ru<sub>6</sub>N]/Al<sub>2</sub>O<sub>3</sub> in H<sub>2</sub> (23.3 kPa), (b) [Ru<sub>6</sub>N]/Al<sub>2</sub>O<sub>3</sub> in <sup>14</sup>N<sub>2</sub> (23.3 kPa), (c) [Ru<sub>6</sub>N]/Al<sub>2</sub>O<sub>3</sub> in <sup>15</sup>N<sub>2</sub> (23.3 kPa), and (d) Al<sub>2</sub>O<sub>3</sub> in <sup>14</sup>N<sub>2</sub> (23.3 kPa). Each background spectrum was for the sample before the introduction of gas. Observed temperature = 193 K. [Ru<sub>6</sub>N]/Al<sub>2</sub>O<sub>3</sub> was evacuated at 813 K and in H<sub>2</sub> at 588 K. Al<sub>2</sub>O<sub>3</sub> was evacuated at 813 K.

peaks remained at the same wavenumbers. The ratio (0.962) for the peak at 1517 (1459) cm<sup>-1</sup> was in accordance with the theoretical ratio  $\nu_{^{15}\text{N}-^{15}\text{N}}/\nu_{^{14}\text{N}-^{14}\text{N}}$  (0.966). No peak was observed around 1450–1520 cm<sup>-1</sup> when 23.3 kPa of <sup>14</sup>N<sub>2</sub> was introduced to MgO (Figure 2f). Hence, the peak at 1517 (1459) cm<sup>-1</sup> can be assigned to N<sub>2</sub>(a) on [Ru<sub>6</sub>N]( $\mu$ -O<sub>su</sub>)<sub>3</sub>. The other three peaks remained at the same positions in Figure 2d–f and appeared only on MgO. Therefore, they should be due to the interactions of N<sub>2</sub> with the MgO surface or a trace amount of impurity gas adsorbed on MgO such as a trace amount of water or hydrocarbons. The amount of N<sub>2</sub>(a) was estimated to be nearly one per [Ru<sub>6</sub>N] cluster by the uptake measurement at 179 K in Table 3.

The IR study on [Ru<sub>6</sub>N]-Cs<sup>+</sup>/MgO in H<sub>2</sub> or N<sub>2</sub> was experimentally difficult because of the strong absorption by the Cs<sup>+</sup>/MgO support (some part of impregnated Cs<sub>2</sub>CO<sub>3</sub> remained undecomposed) and the difficulty to regulate an adequate amount of cluster 1 solution dropped onto the Cs<sup>+</sup>/MgO disk in the IR cell.

**2. [Ru<sub>6</sub>N]/Al<sub>2</sub>O<sub>3</sub>.** The IR observations in H<sub>2</sub> and in N<sub>2</sub> were also performed for [Ru<sub>6</sub>N]/Al<sub>2</sub>O<sub>3</sub>-588H. The IR spectrum at 193 K for 30 min in H<sub>2</sub> (23.3 kPa) had no peak (Figure 3a), indicating H<sub>2</sub> was not adsorbed on [Ru<sub>6</sub>N]/Al<sub>2</sub>O<sub>3</sub> at 193 K. The spectrum for 30 min in <sup>14</sup>N<sub>2</sub> (23.3 kPa) had four peaks (Figure 3b), and two among the four shifted in <sup>15</sup>N<sub>2</sub> (Figure 3c) (from 1661 to 1602 cm<sup>-1</sup>, from 1444 to 1390 cm<sup>-1</sup>). Therefore, the two peaks at 1661 and 1444 cm<sup>-1</sup> can be assigned to N<sub>2</sub>(a). The ratios (0.963–0.964) were in accordance with the theoretical ratio  $\nu_{^{15}\text{N}-^{15}\text{N}}/\nu_{^{14}\text{N}-^{14}\text{N}}$  (0.966). When 23.3 kPa of <sup>14</sup>N<sub>2</sub> was introduced on Al<sub>2</sub>O<sub>3</sub>, two peaks were observed, at 1822 and 1207 cm<sup>-1</sup>. These two peaks were not shifted in Figure 3b–d and appeared only on Al<sub>2</sub>O<sub>3</sub>, probably due to the interactions of N<sub>2</sub> with the Al<sub>2</sub>O<sub>3</sub> surface or trace amount of impurity gas (water or hydrocarbon) adsorbed on the Al<sub>2</sub>O<sub>3</sub> surface. The molar ratio N<sub>2</sub>(a)/[Ru<sub>3</sub>( $\mu$ -O<sub>su</sub>)<sub>3</sub>] was nearly 1 by the uptake measurement at 179 K (Table 3).

**3. In-Situ IR Spectra in N<sub>2</sub> + 3D<sub>2</sub> at 588 K.** In-situ IR spectra were observed for [Ru<sub>6</sub>N]/MgO in N<sub>2</sub> (16 kPa) and D<sub>2</sub> (48 kPa) at 588 K. In the spectrum for 60 min (background spectrum was for the sample before the introduction of reaction gas at 588 K), no absorptions were observed in the  $\nu_{\text{N-D}}$ ,  $\nu_{\text{N-N}}$ , and  $\nu_{\text{Ru-D}}$  regions except for the growth of  $\nu_{\text{O-D}}$  at 2756(s) and 2661(m, br) cm<sup>-1</sup> (exchange of hydroxyl on MgO). After the evacuation of reaction gas at 588 K, 8.7 kPa of ND<sub>3</sub> was

introduced to this sample at 588 K. In the spectrum for 60 min in ND<sub>3</sub>, two new weak peaks were observed at 2540(vw) and 2362(vw) cm<sup>-1</sup>.

## Discussion

The active structures of [Ru<sub>6</sub>N] on MgO, K<sup>+</sup>/MgO, Cs<sup>+</sup>/MgO, and Al<sub>2</sub>O<sub>3</sub> were summarized in Figure 7 in the previous paper.<sup>13</sup> The [Ru<sub>6</sub>N(CO)<sub>16</sub>]<sup>-</sup> was reacted with MgO and transformed to [Ru<sub>6</sub>N(μ-O<sub>su</sub>)<sub>3</sub>] (O<sub>su</sub>, oxygen atom at surface) by the evacuation at 813 K (decarbonylated). The structure was stable and did not change by subsequent treatment in H<sub>2</sub> at 588 K or treatment in N<sub>2</sub> and H<sub>2</sub> at 588 K. Also on Cs<sup>+</sup>/MgO and K<sup>+</sup>/MgO, cluster **1** was transformed to [Ru<sub>6</sub>N(μ-O<sub>su</sub>)<sub>3</sub>] by the evacuation at 673 K and hydrogen treatment at 588 K. In contrast, cluster **1** was cleaved to the trimer [Ru<sub>3</sub>(μ<sub>2</sub>-O<sub>su</sub>)<sub>3</sub>] on Al<sub>2</sub>O<sub>3</sub> by the evacuation at 813 K, and the species were very stable by T<sub>H<sub>2</sub></sub> = 588–773 K. Cluster **3** was transformed to a non-nitrido hexamer [Ru<sub>6</sub>(μ-O<sub>su</sub>)<sub>3-4</sub>] on MgO in vacuum and in H<sub>2</sub> at 623 K. Cluster **2** without interstitial nitrogen readily aggregated to larger Ru particles on MgO during evacuation at 813 K and/or subsequent H<sub>2</sub> treatment at 588 K (*N*<sub>Ru-Ru</sub> = 5.9–6.2).

The TOFs of ammonia synthesis at 588 K were in the following order: [Ru<sub>6</sub>N(μ-O<sub>su</sub>)<sub>3</sub>] on Cs<sup>+</sup>/MgO (0.40 min<sup>-1</sup>) > [Ru<sub>6</sub>N(μ-O<sub>su</sub>)<sub>3</sub>] on K<sup>+</sup>/MgO (0.19) > [Ru<sub>6</sub>N(μ-O<sub>su</sub>)<sub>3</sub>] on MgO (0.11) > [Ru<sub>6</sub>(μ-O<sub>su</sub>)<sub>3-4</sub>] on MgO (0.018) > [Ru<sub>3</sub>(μ<sub>2</sub>-O<sub>su</sub>)<sub>3</sub>] on Al<sub>2</sub>O<sub>3</sub> (0) (Table 1). Aggregated Ru particles from clusters **1** or **2** (*N*<sub>Ru-Ru</sub> = 6.2–6.6) or conventional Ru catalysts on MgO or on Al<sub>2</sub>O<sub>3</sub> exhibited lower activities (0.001–0.017 min<sup>-1</sup>), but still better than the supported triangle cluster on Al<sub>2</sub>O<sub>3</sub> (no activity) (Table 1). Taking into account each active structure, these TOF data are discussed with regard to three control factors over the catalysis: (1) nuclearity of the Ru cluster, (2) cluster/support interface, and (3) nitrido nitrogen.

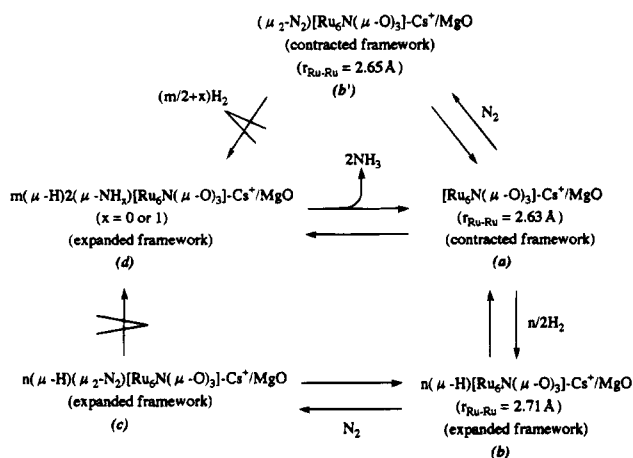
**Nuclearity of the Ruthenium Cluster and Catalysis.** We can compare the effect of nuclearity on catalysis for four samples on MgO which were free from nitrido N in the cluster structure, [Ru<sub>6</sub>C]/MgO-623H, [Ru<sub>6</sub>/MgO-588H, [Ru<sub>6</sub>N]/MgO-773H, and conventional Ru/MgO (Table 1). Supported Ru clusters with six Ru atoms without nitrido N (0.018 min<sup>-1</sup>) were more active than the aggregated Ru clusters (0.013–0.017 min<sup>-1</sup>) and much more active than the conventional one (0.002 min<sup>-1</sup>) (Table 1). The sample [Ru<sub>6</sub>N]/MgO-773H, originally prepared from nitrido cluster **1**, must have lost nitrido N during the hydrogen treatment above 600 K (Figure 5 in the accompanying paper)<sup>13</sup> and aggregated (*N*<sub>Ru-Ru</sub> = 6.6). The activity was nearly equal to that of [Ru<sub>6</sub>/MgO-588H prepared from [Ru<sub>6</sub>(CO)<sub>18</sub>]<sup>2-</sup> (0.013 min<sup>-1</sup>). No activity on triangle Ru cluster [Ru<sub>3</sub>(μ<sub>2</sub>-O<sub>su</sub>)<sub>3</sub>] on Al<sub>2</sub>O<sub>3</sub> should be mainly due to the nature of Al<sub>2</sub>O<sub>3</sub> support. Conventional Ru/Al<sub>2</sub>O<sub>3</sub> could not activate N<sub>2</sub> very well and gave low ammonia synthesis activity (0.001 min<sup>-1</sup>). However, it is interesting to point out that [Ru<sub>3</sub>(μ<sub>2</sub>-O<sub>su</sub>)<sub>3</sub>] on Al<sub>2</sub>O<sub>3</sub> was not able to dissociate H<sub>2</sub> on the basis of IR in H<sub>2</sub> (no adsorption of H) (Figure 3a) and the low exchange rate of H<sub>2</sub>/D<sub>2</sub> (2.0 min<sup>-1</sup>) (Table 1). The poorer ability to activate hydrogen must be another reason for the low TOF in ammonia synthesis. Thus, we cannot discuss the case of the three-Ru-atom ensemble in the same context as hexamer and larger particles. Roughly speaking, the smaller the nuclearity of the cluster, the higher the activity at least up to the size of the six-Ru-atom ensemble. The cluster nuclearity should be related to the support effect because the smaller cluster was more strongly affected by the support. In fact, the TOF on supported [Ru<sub>6</sub>N] was dependent on the Ru wt % (Figure 1) and the kind of support (Table 1). Hence, the discussion should be extended to include the cluster/support interface.

**TABLE 4: IR Absorption Peaks of H(a) on [Ru<sub>6</sub>N(CO)<sub>16</sub>]<sup>-</sup> Clusters Supported on MgO, and IR and Raman Peaks of Related Systems**

	ν/cm <sup>-1</sup>			method	ref
	on-top	bridging	3-fold		
H <sub>2</sub> Ru(CO) <sub>4</sub>	1980			IR	31
H <sub>2</sub> Ru(CO) <sub>2</sub> (PPh <sub>3</sub> ) <sub>2</sub>	1878, 1823			IR	31
Fe-Al <sub>2</sub> O <sub>3</sub> -K <sub>2</sub> O	1954, 1902, 1870			Raman	32
Fe, Co, Ni, Rh, Pd, or Ir on Al <sub>2</sub> O <sub>3</sub>	1940–1850			IR	33
Ru/MgO	1880, 1801, 1717	1550, 1330	1120, 933	IR	34
Ru-Cs <sup>+</sup> /MgO	1781	1540, 1407	1233, 940	IR	34
H <sub>2</sub> Ru <sub>4</sub> (CO) <sub>12</sub>		1585, 1290		Raman	35
H <sub>2</sub> Ru <sub>6</sub> (CO) <sub>18</sub>			708, 660, 652	IR	36
[Ru <sub>6</sub> N(CO) <sub>16</sub> ] <sup>-</sup> /MgO	1944			IR	this work

**Cluster/Support Interface and Catalysis.** The Ru wt % dependence of TOF for ammonia synthesis was shown in Figure 1. The TOF exhibited only a slight change around 1.5–3 wt % Ru, but the TOF increased at 0.48 wt % Ru and decreased at 3.9 wt %. These changes corresponded well to the structure changes of the cluster and cluster/support interface. The aggregation to larger Ru particles was observed by EXAFS (*N*<sub>Ru-Ru</sub> = 5.0) at 3.9 wt % Ru,<sup>13</sup> and this decrease tendency of TOF was in accordance with the change of TOF for [Ru<sub>6</sub>N]/MgO (2.5 wt % Ru) (Table 1) at different reduction temperatures (*N*<sub>Ru-Ru</sub> was 4.1 at T<sub>H<sub>2</sub></sub> = 588 K and 6.6 at T<sub>H<sub>2</sub></sub> = 773 K).<sup>13</sup> The *N*<sub>Ru-O<sub>su</sub></sub> was observed to increase from 0.5 to 1.2 when the Ru wt % decreased from 2.5 to 0.48, keeping the *N*<sub>Ru-Ru</sub> unchanged (4.0 ± 0.1).<sup>13</sup> The increase of TOF at 0.48 wt % Ru must be closely related to the cluster/support interface (number and nature of Ru-O<sub>su</sub> bondings) because the cluster framework structure [Ru<sub>6</sub>N] was kept unchanged.

**Nitrido Nitrogen and Catalysis.** 1. *H-induced Structure Change for Supported [Ru<sub>6</sub>N]*. The TOF on the ruthenium hexamer with nitrido N was larger by 6.1 times than that without nitrido N on MgO (Table 1). In EXAFS measurements, expansion/contraction of the [Ru<sub>6</sub>N] framework was observed as a change of *r*<sub>Ru-Ru</sub> = 2.62 ⇌ 2.65 Å on MgO and 2.63 ⇌ 2.71 Å on Cs<sup>+</sup>/MgO by the adsorption/desorption of hydrogen.<sup>13</sup> In the IR observations, the adsorbed H showed peaks at 1944 cm<sup>-1</sup> in H<sub>2</sub> and at 1374 cm<sup>-1</sup> in D<sub>2</sub> on [Ru<sub>6</sub>N(μ-O<sub>su</sub>)<sub>3</sub>] on MgO (Figure 2). Reported vibrational frequencies are listed in Table 4 for the stretching mode ν<sub>Ru-H</sub> of on-top, bridging, and 3-fold H(a) on metal clusters/complexes and supported catalysts. The on-top H(a)'s on organometallic Ru complexes or conventional metal (Fe, Co, Ni, Ru, Rh, Pd, Ir) catalysts were in the range 1980–1717 cm<sup>-1</sup>.<sup>31-34</sup> The bridging and 3-fold H(a)'s on Ru carbonyl clusters have two vibrational modes, ν<sub>as</sub> and ν<sub>s</sub>, in the range 1585–1290 cm<sup>-1</sup><sup>35</sup> and 708–652 cm<sup>-1</sup>,<sup>36</sup> respectively (Table 4). The amount of H(a) per [Ru<sub>6</sub>N(μ-O<sub>su</sub>)<sub>3</sub>] was estimated to be three to four on [Ru<sub>6</sub>N]/MgO and five to six on [Ru<sub>6</sub>N]-Cs<sup>+</sup>/MgO on the basis of the intensity of the ν<sub>Ru-H</sub> peak and the uptake measurements at 77–193 K (Table 3). There is a tendency for hydrogen to be adsorbed at on-top sites on metal particles of conventional metal catalysts and at bridging or 3-fold sites on organometallic carbonyl Ru clusters in Table 4. However, the hydrogen on organometallic carbonyl clusters is located in the small free space between the bulky carbonyl ligands. Our [Ru<sub>6</sub>N(μ-O<sub>su</sub>)<sub>3</sub>] had metallic *r*<sub>Ru-Ru</sub> (2.62–2.63 Å)<sup>13</sup> shortened from a cluster-like 2.88 Å (determined by EXAFS) of unsupported cluster **1**, and all the carbonyl ligands of cluster **1** desorbed by heating in vacuum. In this context, adsorption of H on [Ru<sub>6</sub>N(μ-O<sub>su</sub>)<sub>3</sub>] as on-top does not contradict with previous reports in Table 4. On the basis of EXAFS and IR data, this reversible change induced by the adsorption/desorption of hydrogen is shown in Scheme 1a,b. The changes

**SCHEME 1: Proposed Reaction Mechanism of Ammonia Synthesis on Supported [Ru<sub>6</sub>N] Clusters**


of  $r_{\text{Ru-Ru}}$  were 1.1% for [Ru<sub>6</sub>N]/MgO and 3.0% for [Ru<sub>6</sub>N]-Cs<sup>+</sup>/MgO.

2. *N<sub>2</sub> Adsorption on Supported [Ru<sub>6</sub>N].* The adsorptions of molecular nitrogen were observed on [Ru<sub>6</sub>N]/MgO-588H and [Ru<sub>6</sub>N]/Al<sub>2</sub>O<sub>3</sub>-588H by IR. The structures of each cluster sample were determined as [Ru<sub>6</sub>N(μ-O<sub>su</sub>)<sub>3</sub>] and [Ru<sub>3</sub>(μ<sub>2</sub>-O<sub>su</sub>)<sub>3</sub>] by EXAFS.<sup>13</sup> For the MgO-supported system, the peak at 1517 cm<sup>-1</sup> in <sup>14</sup>N<sub>2</sub> (1459 cm<sup>-1</sup> in <sup>15</sup>N<sub>2</sub>) (Figure 3) can be assigned as N<sub>2</sub>(a) on [Ru<sub>6</sub>N(μ-O<sub>su</sub>)<sub>3</sub>], judging from the accordance of the isotope shift of the wavenumber with the theoretical value (0.966) and the absence of these peaks for the MgO sample. We believe that the vibration of lying-down N<sub>2</sub> was possible to detect on the dispersed [Ru<sub>6</sub>N] cluster, *not* directly adsorbed on the rather flat MgO surface. In the case of [Ru<sub>6</sub>N]/Al<sub>2</sub>O<sub>3</sub>-588H, two IR peaks were observed, at 1661 and 1444 cm<sup>-1</sup> (1602 and 1390 cm<sup>-1</sup> for <sup>15</sup>N<sub>2</sub>), ascribable to N<sub>2</sub>(a) on [Ru<sub>3</sub>(μ<sub>2</sub>-O<sub>su</sub>)<sub>3</sub>] (Figure 3), judging from the isotope shift and the absence of these peaks for the Al<sub>2</sub>O<sub>3</sub> disk.

On the Fe(111) surface, adsorbed <sup>15</sup>N<sub>2</sub> at lower than 80 K showed an absorption peak at 2100 cm<sup>-1</sup>, and adsorbed <sup>15</sup>N<sub>2</sub> at 100 K showed an absorption peak at 1490 cm<sup>-1</sup> (Table 5).<sup>3,37</sup> The two kinds of N<sub>2</sub>(a) were assigned as on-top and bridging N<sub>2</sub>(a), respectively, by X-ray and ultraviolet photoelectron spectroscopy observations. It should be noted that some part of this bridging N<sub>2</sub>(a) on Fe(111) was transformed to atomic nitrogen on the Fe(111) surface, and the rates of ammonia synthesis at 673 K were in the order Fe(111) > Fe(211) > Fe(100) > Fe(210) > Fe(110),<sup>43</sup> suggesting that the lower coordination Fe face was favorable to ammonia synthesis. Compared with vibrational data in Table 5, peaks on [Ru<sub>6</sub>N]/MgO at 1517 cm<sup>-1</sup> can be assigned as bridging N<sub>2</sub>(a) on [Ru<sub>6</sub>N(μ-O<sub>su</sub>)<sub>3</sub>]. It was suggested that one or two bridging N<sub>2</sub>(a) were coordinated to the [Ru<sub>6</sub>N(μ-O<sub>su</sub>)<sub>3</sub>] cluster on the basis of the  $N_{\text{Ru-N}}$  (0.4–0.7) for N<sub>2</sub>(a) on [Ru<sub>6</sub>N]/MgO and [Ru<sub>6</sub>N]-Cs<sup>+</sup>/MgO observed by EXAFS<sup>13</sup> and uptake measurements of N<sub>2</sub>(a) on [Ru<sub>6</sub>N(μ-O<sub>su</sub>)<sub>3</sub>] (0.7–1.1) in Table 3. Similarly, about one bridging N<sub>2</sub>(a) was coordinated to [Ru<sub>3</sub>(μ<sub>2</sub>-O<sub>su</sub>)<sub>3</sub>] on Al<sub>2</sub>O<sub>3</sub> on the basis of Table 3. Upon the adsorption of N<sub>2</sub> on [Ru<sub>6</sub>N(μ-O<sub>su</sub>)<sub>3</sub>], negligible changes of bond distances for Ru–Ru and Ru–O<sub>su</sub> were observed on MgO and Cs<sup>+</sup>/MgO.<sup>13</sup>

3. *Reaction Mechanism of Ammonia Synthesis.* While no IR peaks were observed in the wavenumber region of  $\nu_{\text{N-D}}$  for [Ru<sub>6</sub>N]/MgO in N<sub>2</sub> + 3D<sub>2</sub> at 588 K, two new peaks were observed, at 2540 and 2362 cm<sup>-1</sup>, in ND<sub>3</sub> at 588 K. Compared to ammonia vibrational data (3444(E), 3337(A<sub>1</sub>), 1627(E), 950(A<sub>1</sub>) for NH<sub>3</sub> and 2564, 2420, 1191, 748 cm<sup>-1</sup> for ND<sub>3</sub>)<sup>44</sup> and reported data for NH<sub>2</sub>(a) (3380, 3290, 1610 cm<sup>-1</sup>) and NH(a) (3200 cm<sup>-1</sup>) on Fe/SiO<sub>2</sub>,<sup>45</sup> these two peaks can be assigned as

ND<sub>2</sub>(a) on [Ru<sub>6</sub>N(μ-O<sub>su</sub>)<sub>3</sub>]. It is interesting that NH<sub>2</sub>(a) formation was reported on the stepped (coordinatively less saturated) Ru(1,1,10) surface, but *not* on the flat Ru(001) surface,<sup>46</sup> compared to our case of unsaturated supported clusters [Ru<sub>6</sub>N(μ-O<sub>su</sub>)<sub>3</sub>]. NH<sub>3</sub> was molecularly adsorbed on Ru(001) and Ru(1,1,10) surfaces at 120 K. By the subsequent heating to 300 K, the NH<sub>3</sub>(a) was transformed to NH<sub>2</sub>(a) on the Ru(1,1,10) surface, as confirmed by the binding energies of N 1s (398.1 eV) in XPS and of valence level (7.4, ~10 eV) in UPS, although only the desorption of NH<sub>3</sub> was observed on Ru(001) surface.<sup>46</sup> In other words, higher ability to activate the NH<sub>x</sub> species was suggested on stepped (unsaturated) Ru(1,1,10) surfaces than flat (001) surfaces.

Inverse D<sub>2</sub>/H<sub>2</sub> isotope effects were observed for [Ru<sub>6</sub>N]/MgO and [Ru<sub>6</sub>N]-Cs<sup>+</sup>/MgO ( $r_{\text{D}_2}/r_{\text{H}_2} = 1.4\text{--}1.5$ ), but no isotope effect was observed for conventional Ru/MgO (Table 2). The total ammonia synthesis reaction rate can be formulated on the basis of the Langmuir equation and classified according to the main surface species during catalysis (whose residence times on the Ru cluster surface are longer than the other species) on the Ru surface in the following reaction conditions: (i) NH<sub>x</sub>(a) (x = 0, 1, 2, 3) was the main surface species, and (ii) H(a) was the main surface species.<sup>47</sup>

$$r = kP_{\text{N}_2}/\{1 + K^{-1}P_{\text{NH}_3}/P_{\text{H}_2}^{(3-x)/2}\}^2 \quad (\text{i})$$

$$r = kP_{\text{N}_2}/(1 + K^{1/2}P_{\text{H}_2}^{1/2})^2 \quad (\text{ii})$$

The *in-situ* IR observation in N<sub>2</sub> + 3D<sub>2</sub> showed no peaks of adsorbates (*or* intermediate species), while two peaks corresponding to ND<sub>2</sub>(a) were observed in ND<sub>3</sub> at 588 K. Hence, we can exclude the possibility that NH<sub>2</sub>(a) or NH<sub>3</sub>(a) was the main surface species during the synthesis reaction. The equilibrium constant  $K$  in the above equation is for the step N(a) + (3/2)H<sub>2</sub> ⇌ NH<sub>3</sub> in the case where N(a) was the main surface species, and the ratio of  $K_{\text{D}_2}/K_{\text{H}_2}$  was calculated on the basis of the vibrational partition function<sup>48</sup> with vibrational data for ammonia (listed above) and the hydrogen molecule ( $\nu_{\text{H-H}} = 4161$ ,  $\nu_{\text{D-D}} = 2993$  cm<sup>-1</sup>).<sup>44</sup>

$$K_{\text{D}_2}/K_{\text{H}_2} = \exp\left\{-\sum(\nu_{\text{N-D}}(\text{ND}_3) - \nu_{\text{N-H}}(\text{NH}_3)) + 3/2(\nu_{\text{D-D}} - \nu_{\text{H-H}})\right\}/h/2kT = 12 \quad (1)$$

In the case where NH(a) was the main surface species, the equilibrium constant in question is for the step NH(a) + H<sub>2</sub> ⇌ NH<sub>3</sub>, and the ratio was calculated similarly.

$$K_{\text{D}_2}/K_{\text{H}_2} = \exp\left\{-\sum(\nu_{\text{N-D}}(\text{ND}_3) - \nu_{\text{N-H}}(\text{NH}_3)) + (\nu_{\text{N-D}}(\text{ND}) - \nu_{\text{N-H}}(\text{NH})) + (\nu_{\text{D-D}} - \nu_{\text{H-H}})\right\}/h/2kT = 8.2 \quad (2)$$

The value of  $K$  in the case where H(a) was the main surface species is for the step H<sub>2</sub> ⇌ 2H(a), and the ratio was calculated with  $\nu_{\text{Ru-H}} = 1944$ ,  $\nu_{\text{Ru-D}} = 1374$  cm<sup>-1</sup> (Figure 2),  $\nu_{\text{H-H}}$ , and  $\nu_{\text{D-D}}$ .

$$K_{\text{D}_2}/K_{\text{H}_2} = \exp\left\{-2(\nu_{\text{Ru-D}} - \nu_{\text{Ru-H}}) + (\nu_{\text{D-D}} - \nu_{\text{H-H}})\right\}/h/2kT = 0.97 \quad (3)$$

Therefore, the observed inverse isotope effects for [Ru<sub>6</sub>N]/MgO and [Ru<sub>6</sub>N]-Cs<sup>+</sup>/MgO can be explained when the dissociated N(a) or NH(a) was the main surface species on Ru atoms of [Ru<sub>6</sub>N(μ-O<sub>su</sub>)<sub>3</sub>] clusters with the  $K$  values 8–12 in eq 1 or 2. In contrast, no isotope effect for conventional Ru/MgO was consistent with almost the same value of  $K$  as unity (0.97) in

**TABLE 5: IR Absorption Peaks of N<sub>2</sub> Adsorbed on [Ru<sub>6</sub>N(CO)<sub>16</sub>]<sup>-</sup> Clusters Supported on MgO and Al<sub>2</sub>O<sub>3</sub>, and IR and EELS (Electron Energy Loss Spectroscopy) Peaks of Related Systems**

	$\nu/\text{cm}^{-1}$		method	ref
	on-top	bridging		
CoH(N <sub>2</sub> )(PPh <sub>3</sub> ) <sub>3</sub>	2085		IR	38
RuH <sub>2</sub> (N <sub>2</sub> )(PPh <sub>3</sub> ) <sub>3</sub>	2147		IR	39
Ru/Al <sub>2</sub> O <sub>3</sub>	2268, 2214		IR	40
Ru-Cs <sup>+</sup> /Al <sub>2</sub> O <sub>3</sub>	2095		IR	40
Ru/MgO	2154		IR	34
Ru-Cs <sup>+</sup> /MgO	2120, 2020		IR	34
ReCl(PMe <sub>2</sub> Ph) <sub>4</sub> -N <sub>2</sub> -MoCl <sub>2</sub> (OMe)	1660		IR	41
( $\mu_3$ -N <sub>2</sub> )[( $\eta^2$ : $\eta^5$ -C <sub>10</sub> H <sub>8</sub> )( $\eta$ -Cp) <sub>2</sub> Ti <sub>2</sub> ] <sup>+</sup> [( $\eta^1$ : $\eta^5$ -C <sub>5</sub> H <sub>4</sub> )-( $\eta$ -Cp) <sub>3</sub> Ti <sub>2</sub> ] <sup>+</sup> ( $\eta$ -Cp) <sub>2</sub> (C <sub>6</sub> H <sub>14</sub> O <sub>3</sub> )Ti <sup>+</sup> ·C <sub>6</sub> H <sub>14</sub> O <sub>3</sub>		1282	IR	42
Fe(111)	2100 <sup>a</sup>	1490 <sup>a</sup>	EELS	37
K-doped Fe(111)		1370 <sup>a</sup>	EELS	43
[Ru <sub>6</sub> N(CO) <sub>16</sub> ] <sup>-</sup> /MgO		1517	IR	this work
[Ru <sub>6</sub> N(CO) <sub>16</sub> ] <sup>-</sup> /Al <sub>2</sub> O <sub>3</sub>		1661, 1444	IR	this work

<sup>a</sup> For <sup>15</sup>N<sub>2</sub>.**TABLE 6: IR Absorption Peaks of CO Adsorbed on [Ru<sub>6</sub>N(CO)<sub>16</sub>]<sup>-</sup>, [Ru<sub>6</sub>C(CO)<sub>16</sub>Me]<sup>-</sup>, and [Ru<sub>6</sub>(CO)<sub>18</sub>]<sup>2-</sup> Clusters Supported on MgO and Conventional Ru/MgO Catalysts**

precursor Ru wt %	$\nu/\text{cm}^{-1}$				
	[Ru <sub>6</sub> N(CO) <sub>16</sub> ] <sup>-</sup>		[Ru <sub>6</sub> C(CO) <sub>16</sub> Me] <sup>-</sup>	[Ru <sub>6</sub> (CO) <sub>18</sub> ] <sup>2-</sup>	Ru(NO)(NO <sub>3</sub> ) <sub>3</sub>
	2.5	0.06	1.8	2.5	2.5
	2059w(sh)	1978w(sh)	2045w(sh)	2069w(sh)	2010s(br)
	2045w(sh)	1965s	1989s	2006s	
	1992s		1933w(sh)	1925w(sh)	
			1795w(br)		

eq 3. In the IR study,<sup>34</sup> no adsorption of N<sub>2</sub> was reported on conventional Ru/MgO (183 K) or Ru-Cs<sup>+</sup>/MgO (293 K) in N<sub>2</sub> + H<sub>2</sub> (8.2 kPa) due to the stronger occupation of surface Ru sites by H(a). The N<sub>2</sub> adsorption ( $\theta_{\text{N}_2}$ ) was only 8.0 and 1.3% on H-preadsorbed conventional Ru/MgO (183 K) and Ru-Cs<sup>+</sup>/MgO (293 K) in N<sub>2</sub> (1.5 kPa) compared to a  $\theta_{\text{H}}$  of 65 and 50%, respectively, although the values might be lower at elevated temperature during catalysis. Thus, main surface species on conventional Ru/MgO or Ru-Cs<sup>+</sup>/MgO should be H(a), which had no H<sub>2</sub>/D<sub>2</sub> isotope effect (Table 2).

The proposed reaction mechanism on supported [Ru<sub>6</sub>N( $\mu$ -O<sub>su</sub>)<sub>3</sub>] cluster is illustrated in Scheme 1 based on *in-situ* EXAFS,<sup>13</sup> IR for adsorbed H and N<sub>2</sub>, the N<sub>2</sub> pressure dependence ( $0.84 \pm 0.06$ ), and inverse isotope effects of H/D on ammonia synthesis. We propose two possibilities of reaction cycles according to the order of adsorptions of H<sub>2</sub> and N<sub>2</sub>. Hydrogen adsorption was in very fast equilibrium compared to steady state ammonia synthesis on the basis of the higher H<sub>2</sub>-D<sub>2</sub> exchange rates, even in the presence of N<sub>2</sub> on supported [Ru<sub>6</sub>N( $\mu$ -O<sub>su</sub>)<sub>3</sub>] clusters (Table 1). The equilibrium step (species (a)  $\rightleftharpoons$  (b)) should be accompanied by cluster expansion/contraction observed as the change of  $r_{\text{Ru-Ru}}$  ( $2.63 \rightleftharpoons 2.71$  Å on Cs<sup>+</sup>/MgO and  $2.62 \rightleftharpoons 2.65$  Å on MgO) by the adsorption/desorption by means of EXAFS.<sup>13</sup> The N<sub>2</sub> can be adsorbed on species (b) as  $\mu_2$ -bridging style on [Ru<sub>6</sub>N( $\mu$ -O<sub>su</sub>)<sub>3</sub>] to be species (c) on the basis of the wavenumber of N<sub>2</sub>(a) in IR spectra (Figure 2d,e) and EXAFS in N<sub>2</sub>,<sup>13</sup> keeping the expanded cluster framework, although the concentration might be low at elevated temperature during catalysis. The main surface species during the catalysis should be N(a) or NH(a) on the basis of the inverse H<sub>2</sub>/D<sub>2</sub> isotope effects (Table 2) and calculations of equilibrium constants in N<sub>2</sub> + 3H<sub>2</sub> or in N<sub>2</sub> + 3D<sub>2</sub> at 588 K (eqs 1 and 2). Compared to the relatively stable species (d), progressive steps of hydrogenation of NH<sub>2</sub>(a) and desorption of NH<sub>3</sub>(a) should be very fast, similar to the equilibrium of H<sub>2</sub> adsorption between species (a) and (b), and contracted species (a) was reproduced (route 1).

The second possible route is through the adsorption of N<sub>2</sub> on [Ru<sub>6</sub>N( $\mu$ -O<sub>su</sub>)<sub>3</sub>], keeping the contracted framework, as in

species (b'). The structure was based on the EXAFS measurement in N<sub>2</sub> ( $r_{\text{Ru-Ru}} = 2.65$ ,  $r_{\text{Ru-O}_{\text{su}}} = 2.07$ ,  $r_{\text{Ru-N}} = 2.02$  Å).<sup>13</sup> Subsequently, the H<sub>2</sub> can be dissociatively adsorbed to be species (d). The cluster should be expanded by the adsorption of H, and the expansion can promote the dissociation of N<sub>2</sub>(a) to N(a) or NH(a) by elongating the Ru-Ru distance (route 2). In these two possible routes (Scheme 1), the structural contribution was suggested for the promotions of hydrogen adsorption (route 1) or nitrogen dissociation (route 2). The supported [Ru<sub>6</sub>( $\mu$ -O<sub>su</sub>)<sub>3-4</sub>] did not show H-induced structure change, keeping  $r_{\text{Ru-Ru}} = 2.63$  Å unchanged ( $N = 4.0 \pm 0.3$ ).<sup>13</sup>

The expansion/contraction of the cluster framework was also reported by the CO adsorption/desorption for [Ru<sub>6</sub>C], and it became possible when catalysts were in CO + H<sub>2</sub> at elevated temperature (473–523 K), as observed by the change of EXAFS ( $\Delta r_{\text{Ru-Ru}}$ ) and the CO uptake.<sup>30</sup> In the case of [Ru<sub>6</sub>C]/MgO, the  $r_{\text{Ru-Ru}}$  changed reversibly between 2.63 and 2.87 Å and CO-(a)/[Ru<sub>6</sub>C] (molar ratio) was 2.9 at 290 K and 10.7 at 523 K. The temperature range where the cluster expansion/contraction was observed coincided with the catalytic reaction temperature, but the reported expansion/contraction did not necessarily correspond to elementary steps in overall catalysis because the adsorption of CO should be very strong even around 473–523 K, and the [Ru<sub>6</sub>C] framework may always be expanded by CO-(a) in reaction conditions of CO/H<sub>2</sub>. At least it was valid that the catalysis was promoted by the elongated Ru-Ru which was covered by CO(a) and by facilitating the dissociative adsorption of H<sub>2</sub>. In this paper, the [Ru<sub>6</sub>N] clusters also exhibited framework expansion/contraction by the adsorption/desorption of H, but the temperature range did not correspond to the reaction temperature of catalysis. We would like to point out the possibility that the expansion/contraction of the [Ru<sub>6</sub>N] framework was incorporated as an elementary step of the overall reaction in Scheme 1, similar to the promoted reactions in refs 22–25, because the population of species (b), (c), or (b') should be low at elevated temperatures during catalysis. The strong coordination of N<sub>2</sub> (as  $\mu_2$ -style) was suggested by EXAFS and IR on [Ru<sub>6</sub>N( $\mu$ -O<sub>su</sub>)<sub>3</sub>], but only on-top ( $\mu_1$ ) N<sub>2</sub>(a) was observed on conventional Ru/MgO and Ru-Cs<sup>+</sup>/MgO (Ru particle size

~ 30 Å) (Table 5).<sup>34</sup> The promoted catalysis was possible when N<sub>2</sub> was strongly adsorbed as μ<sub>2</sub>-style. This difference may be the main factor which made smaller clusters (n = 6) more favorable to ammonia synthesis.

**4. Chemical Effect of Nitrido Nitrogen.** It is impossible to distinguish the structural and chemical effects of nitrido nitrogen because structural effects (cluster expansion/contraction and change of coordination style of N<sub>2</sub>(a)) were only observed in the system with nitrido nitrogen, i.e. supported [Ru<sub>6</sub>N(μ-O<sub>su</sub>)<sub>3</sub>] clusters on MgO and Cs<sup>+</sup>/MgO. Prepared supported [Ru<sub>6</sub>(μ-O<sub>su</sub>)<sub>3-4</sub>] did not have nitrido nitrogen nor H-induced cluster expansion/contraction.

A general comparison of the carbonyl frequencies is listed in Table 6 for MgO-supported Ru clusters (pretreated in the same procedure as for ammonia synthesis) in CO. The stretching vibration wavenumber ν<sub>CO</sub> for [Ru<sub>6</sub>N]/MgO (2.5 wt %) was similar to [Ru<sub>6</sub>C]/MgO<sup>30</sup> and smaller than that for aggregated [Ru<sub>6</sub>]/MgO (N<sub>Ru-Ru</sub> = 6.2) or conventional Ru/MgO catalyst by 14–18 cm<sup>-1</sup>. The difference became larger in the case of [Ru<sub>6</sub>N]/MgO at 0.06 wt % Ru (41–45 cm<sup>-1</sup>). On the basis of the EXAFS analysis in the previous paper,<sup>13</sup> cluster 1 always maintained the [Ru<sub>6</sub>N] unit upon supporting (T<sub>H<sub>2</sub></sub> < 623 K), contrary to the change of the number x (change of adsorption site on MgO). Thus, although there are several factors for the IR wavenumber shifts, these red-shifts of ν<sub>CO</sub> for [Ru<sub>6</sub>N] and [Ru<sub>6</sub>C] on MgO may be ascribed to total electron donation by nitrido N<sup>49</sup> and by support MgO, which were larger than general ν<sub>CO</sub> shifts induced by the change of Ru particle size on support.<sup>50</sup> The promotion of N<sub>2</sub> dissociation by electron donors to metal active sites is widely known.<sup>26,29,48</sup>

## Conclusions

1. Supported [Ru<sub>6</sub>N(μ-O<sub>su</sub>)<sub>3</sub>] clusters on MgO, K<sup>+</sup>/MgO, or Cs<sup>+</sup>/MgO were found to be active for ammonia synthesis.

2. The TOF (per cluster) of ammonia synthesis was larger by ~30% at 0.5 wt % Ru than that at 2.5 wt % for [Ru<sub>6</sub>N]/MgO. Cluster/support interface should be the major factor on the basis of the N<sub>Ru-O<sub>su</sub></sub> of 1.2 (0.5 wt %) and 0.5 (2.5 wt %) below the common [Ru<sub>6</sub>N] species.

3. During ammonia synthesis on supported [Ru<sub>6</sub>N(μ-O<sub>su</sub>)<sub>3</sub>] clusters, N(a) or NH(a) was suggested to be the main surface species on the basis of IR and H/D isotope effects (r<sub>D<sub>2</sub></sub>/r<sub>H<sub>2</sub></sub> = 1.4–1.5), compared to conventional Ru catalysts on whose Ru surface H(a) should predominantly adsorb.

4. New promoted catalysis was suggested on [Ru<sub>6</sub>N] clusters. Compared to the strong adsorption of hydrogen for conventional Ru catalysts on which no H/D isotope effect was observed, the structural promotion of adsorption of H<sub>2</sub> and/or dissociation of N<sub>2</sub> was suggested. The μ<sub>2</sub>-style adsorption of N<sub>2</sub> on [Ru<sub>6</sub>N(μ-O<sub>su</sub>)<sub>3</sub>] may be related to promoted catalysis compared to on-top N<sub>2</sub>(a) on conventional Ru catalysts.

5. Chemical promotion was also implied as the electron donation by nitrido nitrogen.

## References and Notes

- (1) *Hydrogen Effects in Catalysis, Fundamentals and Practical Applications*; Paal, Z., Menon, P. G., Eds.; Marcel Dekker: New York, 1988.
- (2) Christmann, K. *Surf. Sci. Rep.* **1988**, *9*, 1.
- (3) Ertl, G. In *Catalytic Ammonia Synthesis, Fundamentals and Practice*; Jennings, J. R., Ed.; Plenum Press: New York, 1991; p 109.
- (4) Held, G.; Pfnür, H.; Menzel, D. *Surf. Sci.* **1992**, *271*, 21.
- (5) Solokowski, M.; Koch, T.; Pfnür, H. *Surf. Sci.* **1991**, *243*, 261.
- (6) Feulner, P.; Menzel, D. *Surf. Sci.* **1985**, *154*, 465.

- (7) Conrad, H.; Scala, R.; Stenzel, W.; Unwin, R. *J. Chem. Phys.* **1984**, *81*, 6371.
- (8) Barteau, M. A.; Broughton, J. Q.; Menzel, D. *Surf. Sci.* **1983**, *133*, 443.
- (9) Teichner, S. J. In *New Aspects of Spillover Effect in Catalysis*; Inui, Fujimoto, Uchiyama, Masai, Eds.; Elsevier: Amsterdam, The Netherlands, 1993; p 27.
- (10) Connor, W. C., Jr.; Pajonk, G. M.; Teichner, S. J. *Adv. Catal.* **1986**, *34*, 1.
- (11) Bhatia, S.; Engelke, F.; Pruski, M.; Gerstein, B. C.; King, T. S. *J. Catal.* **1994**, *147*, 455.
- (12) Uner, D. O.; Pruski, M.; Gerstein, B. C.; King, T. S. *J. Catal.* **1994**, *146*, 530.
- (13) Izumi, Y.; Aika, K. *J. Chem. Phys.* **1995**, *99*.
- (14) Sheu, L. L.; Knözinger, H.; Sachtler, W. M. H. *Catal. Lett.* **1989**, *2*, 129.
- (15) Sheu, L. L.; Knözinger, H.; Sachtler, W. M. H. *J. Am. Chem. Soc.* **1989**, *111*, 8125.
- (16) Yin, Y.; Zhang, Z.; Sachtler, W. M. H. *J. Catal.* **1993**, *139*, 444.
- (17) Zhang, Z.; Lerner, B.; Lei, G.; Sachtler, W. M. H. *J. Catal.* **1993**, *140*, 481.
- (18) Karpiński, Z.; Gandhi, S. N.; Sachtler, W. M. H. *J. Catal.* **1993**, *141*, 337.
- (19) Van Zon, F. B. M.; Maloney, S. D.; Gates, B. C.; Koningsberger, D. C. *J. Am. Chem. Soc.* **1993**, *115*, 10317.
- (20) Kamper, F. W. H.; Koningsberger, D. C. *Faraday Discuss. Chem. Soc.* **1990**, *89*, 137.
- (21) Vaarkamp, M.; Modica, F. S.; Miller, J. T.; Koningsberger, D. C. *J. Catal.* **1993**, *144*, 611.
- (22) Muetterties, E. L.; Krause, M. J. *Angew. Chem., Int. Ed. Engl.* **1983**, *22*, 135.
- (23) Süß-Funk, G.; Herrmann, G. *J. Chem. Soc., Chem. Commun.* **1985**, 735.
- (24) Daroda, R. J.; Blackborow, J. R.; Wilkinson, G. *J. Chem. Soc., Chem. Commun.* **1980**, 1101.
- (25) Iwasawa, Y. *Catal. Today* **1993**, *18*, 21.
- (26) Aika, K.; Takano, T.; Murata, S. *J. Catal.* **1992**, *136*, 126.
- (27) Nobile, A., Jr.; Brunt, V. V.; Davis, M. W., Jr. *J. Catal.* **1991**, *127*, 227.
- (28) Cisneros, M. D.; Lunsford, J. H. *J. Catal.* **1993**, *141*, 191.
- (29) Tennison, S. R. In *Catalytic Ammonia Synthesis, Fundamentals and Practice*; Jennings, J. R., Ed.; Plenum Press: New York, 1991; p 303.
- (30) Izumi, Y.; Chihara, T.; Yamazaki, H.; Iwasawa, Y. *J. Phys. Chem.* **1994**, *98*, 594.
- (31) Kaesz, H. D.; Saillant, R. B. *Chem. Rev.* **1972**, *72*, 231.
- (32) Zhang, H.; Schrader, G. L. *J. Catal.* **1986**, *99*, 461.
- (33) Kartaradze, N. K.; Sokolova, N. P. *Russ. J. Phys. Chem.* **1970**, *44*, 1485.
- (34) Izumi, Y.; Hoshikawa, M.; Aika, K. *Bull. Chem. Soc. Jpn.* **1994**, *67*, 3191.
- (35) Knox, S. A. R.; Koepke, J. W.; Andrews, M. A.; Kaesz, H. D. *J. Am. Chem. Soc.* **1975**, *97*, 3942.
- (36) Andrews, J. A.; Jayasooriya, U. A.; Oxtan, I. A.; Powell, D. B.; Sheppard, N.; Jackson, P. F.; Johnson, B. F. G.; Lewis, J. *Inorg. Chem.* **1980**, *19*, 3033.
- (37) Tsai, M. C.; Seip, U.; Bassignana, I. C.; Kupperts, J.; Ertl, G. *Surf. Sci.* **1985**, *155*, 387.
- (38) Davis, B. R.; Payne, N. C.; Ibers, J. A. *J. Am. Chem. Soc.* **1969**, *91*, 74.
- (39) Knoth, W. H. *J. Am. Chem. Soc.* **1972**, *94*, 104.
- (40) Kubota, J.; Aika, K. *J. Phys. Chem.* **1994**, *98*, 11293.
- (41) Mercer, M. J. *Chem. Soc., Dalton Trans.* **1974**, 1637.
- (42) Pez, G. P.; Apgar, P.; Crissey, R. K. *J. Am. Chem. Soc.* **1982**, *104*, 482.
- (43) Strongin, D. R.; Carrazza, J.; Bare, S. R.; Somorjai, G. A. *J. Catal.* **1987**, *103*, 213.
- (44) *Chemistry Handbook (Basic Edition)*, 4th ed.; The Chemical Society of Japan, Ed.; Maruzen: Tokyo, 1993.
- (45) Nakata, T.; Matsushima, S. *J. Phys. Chem.* **1968**, *72*, 458.
- (46) Egawa, C.; Naito, S.; Tamaru, K. *Surf. Sci.* **1984**, *138*, 279.
- (47) Aika, K.; Kurmasaka, M.; Oma, T.; Kato, O.; Matsuda, H.; Watanabe, N.; Yamazaki, K.; Ozaki, A.; Onishi, T. *Appl. Catal.* **1986**, *28*, 57.
- (48) Ozaki, A.; Aika, K. In *A Treatise on Dinitrogen Fixation*; Hardy, Bottemely, Burns, Eds.; John Wiley, & Sons, Inc.: New York, 1979; Sections I and II, pp 169–247.
- (49) Bradley, J. S. *Adv. Organomet. Chem.* **1983**, *22*, 1.
- (50) Dalla, Betta, R. A. *J. Phys. Chem.* **1975**, *79*, 2519.